MODELLING THE PHASE BOUNDARIES AND FLUID PROPERTIES OF THE SYSTEM H_2O-NACL AT HIGH TEMPERATURES AND PRESSURES

R. MCKIBBIN[1] AND A. MCNABB[1,2]

'Department of Mathematics, Massey University, Palmerston North
[2]Maths Physics Research Limited, Palmerston North

ABSTRACT - This paper describes a prototype program modelling the state-space of the two-component system H_2O-NaCl over a wide range of temperatures and pressures [$0 < T < 1075$ ˚C, $0 < p < 1600$ bars abs]. Using experimental data from a number of sources, a description is given of the surfaces which divide the three-dimensional T-p-X state-space into its eight regions, each corresponding to one of the various possible equilibrium regimes of fluid-solid states. Approximate correlations, which are based on the primary variables temperature T, pressure p and the mass fraction of chloride **X** in the solution, and which delineate these regional boundaries, are given here; the correlations are being implemented in a subroutine suitable for use within a numerical reservoir simulator.

1. INTRODUCTION

Our interest in the system H_2O-NaCl arises from questions concerning the nature of geothermal chloride waters at depth in geothermal fields, of the kind of fluid present between cooling volcanic magma releasing chloride-saturated magmatic vapours into ground-water at depth in the Earth's crust (McNabb, 1992), and about convecting hydrothermal systems on the sea floor. How is heat transferred to the base of such geothermal systems and how do the fluid phase properties of brines influence the heat transfer and mineral transport?

When dealing with these questions, it is important to remember that temperatures and pressures at the magma surface in these systems are very much above the critical point of pure water ($T_{crit} = 374.15$ ˚C, $p_{crit} = 221.2$ bars), and that the magmatic vapour interacting with the system often has a high chemical content of dissolved salts, minerals and gases which, during cooling, may produce one, two or even more co-existing fluid phases and perhaps some solid phase precipitates, all in local equilibrium.

In order to model such fluids, it is necessary to first delineate their various solid, liquid and vapour phases, the compositions of co-existing phases and their thermodynamic and relevant physical properties, before applying the standard conservation laws to describe the physical evolution of the system. Fortunately, a literature search turned up a number of publications which give conceptual descriptions and experimental data for the H_2O-NaCl system (Sourirajan & Kennedy, 1962; Haas, 1976; Chou, 1987; Bischoff & Pitzer, 1989; Bischoff, 1991) and for the H_2O-NaCl-CO_2 system (Bowers & Helgeson, 1983; Anderson *et al.*, 1992).

The conceptual models of the T-p-X state-space, based on the physical chemistry of the mixtures, were perused, collated, amalgamated and synthesised to gain an understanding of the complicated phase structure of the T-p-X diagrams and describe mathematically the boundaries between regimes within the system.

It was decided to first concentrate on the H_2O-NaCl system, since the addition of C02 makes for enormous complexity. What follows, then, is a treatment of the binary system where water (H_2O) and common salt (NaCl) co-exist, either as a solution of salt in water in liquid or gas form, or as two fluid phases in equilibrium, or even as fluid phases in equilibrium with solid salt precipitate.

2. THE SYSTEM H_2O-NaCl

H_2O-NaCl is a binary system in which solubility of halite in the vapour can be considerable. The behaviour of the system at low temperatures and pressures is not of great interest in the studies outlined earlier and so the phase complications involving ice are ignored, although our diagrams do incorporate the triple point of pure H20 at approximately (0 ˚C, 0 bars) and that for pure NaCl near (800 ˚C, 0 bars) as useful reference points [note: pressures are given in bars absolute].

The mass fraction of NaCl in the binary system is represented by the dimensionless quantity X, where $X = 0$ corresponds to pure H20 and $X = 1$ to pure NaCl. Between these limits, the system can exist in a variety of states, corresponding to various combinations of liquid, gas and solid (NaCl). The phase rule prevails of course, and gives the dimensionality of the various regions and their boundaries in the T-p-X diagram in terms of the number of co-existing phases and components.

Figures 1(a) and (b) show parts of the model T-p-X state-space, which is described in detail below. Figures 2 to 7 show graphs of some experimental data from the literature together with plots of approximate correlations. The correlation formulas, given in the Appendix to this paper, were devised so that any chosen state-point could be classified and allocated to one of the eight regions of the state-space by direct calculation rather than by data table interpolation.

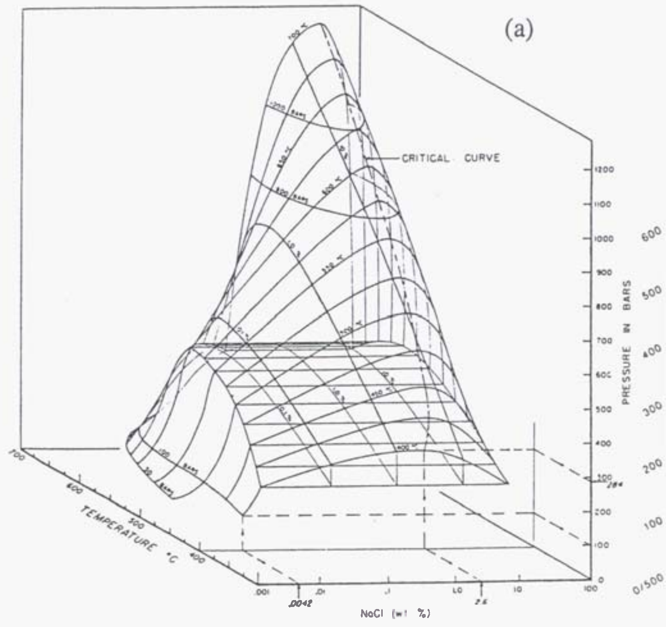

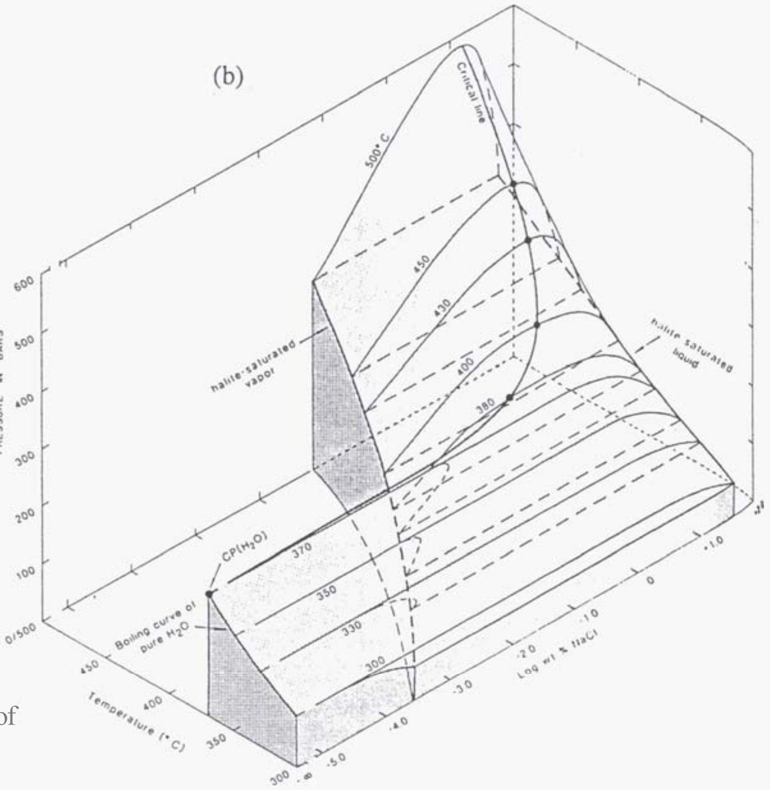

Figure 1. Perspective views of parts of a T-p-X model of the system H_2O-NaCl.
(a) (above) between 400 and 700 "C (after Sourirajan & Kennedy, 1962);
(b) (right) the gas-liquid interface between 300 and 500 "C (after Bischoff & Pitzer, 1989).
(Note the logarithm axis for **X** in each case.)

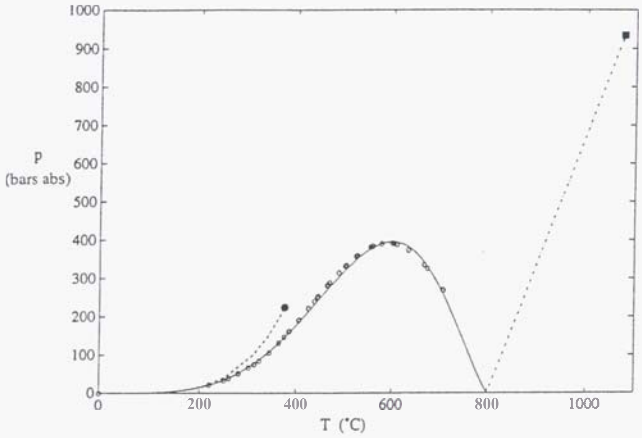

Figure 2. Correlation for the saturation curve $p = p_{SAT}(T)$, the vapour pressure of saturated H_2O-NaCl solutions.
(————) $p = p_{SAT}(T)$;
(– – – –) $p = p_{sat}(T)$: saturation line for pure H_2O;
(– . – . –) $p = p_{sat}(T)$: saturation line for pure NaCl;
(o) data from Sourirajan & Kennedy (1962);
(●) the critical point for pure H_2O;
(■) the critical point for pure NaCl.

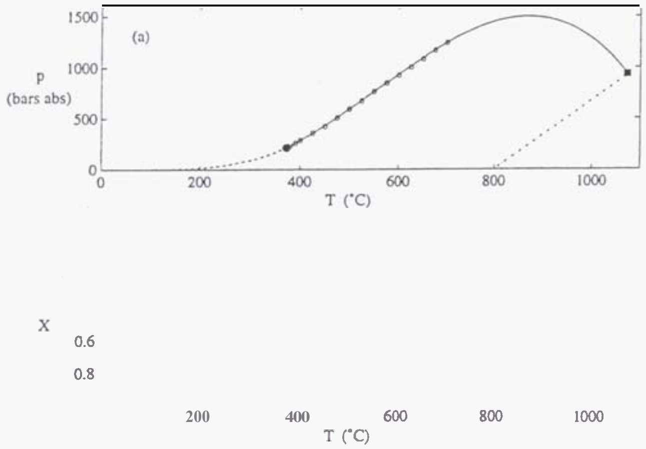

Figure 3. Correlations for the critical curve, from the critical point for pure H20 (●) to that for pure NaCl (■).
(a) (————) $p = p_{CRIT}(T)$;
(– – – –) $p = p_{sat}(T)$: saturation line for pure H_2O;
(– . – . –) $p = p_{sat}(T)$: saturation line for pure NaCl;
(b) (————) $X = X_{CRIT}(T)$;
(o) data from Sourirajan & Kennedy (1962).

The liquid-gas region extends over a large field, It is bounded at low pressures by halite solubility in co-existing liquid and gas (three-phase state), the saturation curve, given by $\mathbf{p} = p_{SAT}(T)$, which extends from near (0 "C, 0 bars) to a maximum pressure at (600 "C, 392 bars) and then descends to the triple point of pure NaCl near (800 "C, 0 bars) (see Figure 2).

At high pressures, the two-phase region is bounded by the saturation curve for pure H_2O, extending from the triple point of H20 to its critical point (374.15 "C, 221.2 bars) (Rogers & Mayhew, 1980), and thence by the H_2O-NaCl critical curve, given by $\mathbf{p} = p_{CRIT}(T)$, which terminates at the critical point for pure NaCl (see Figure 3). While Bischoff & Pitzer (1989) estimate this last point to be near

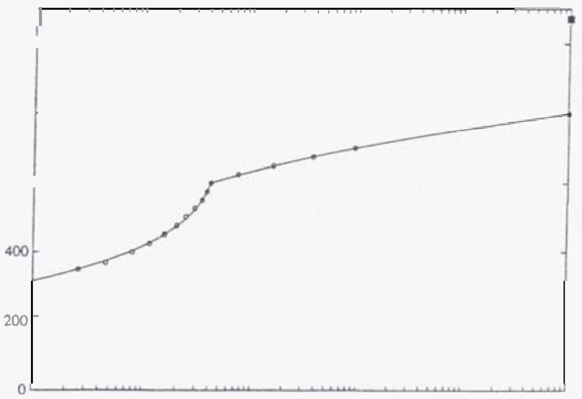

Figure **4.** Correlation for $X = X_{g\ SAT}(T)$, the mass fraction of NaCl in halite-saturated gas.
(———) $X = X_{g\ SAT}(T)$;
(o) data from Sourirajan & Kennedy (1962);
(■) the critical point for pure NaCl.

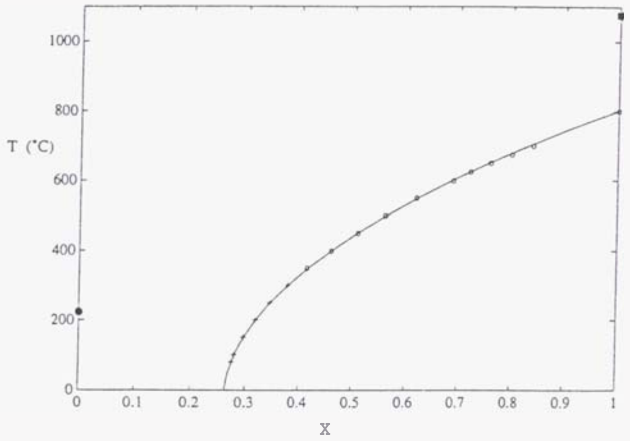

Figure 5. Correlation for $X = X_{\ell\ SAT}(T)$, the mass fraction of NaCl in saturated liquid
(———) $X = X_{\ell\ SAT}(T)$;
(o) data from Sourirajan & Kennedy (1962);
(+) data from Haas (1976);
(●) the critical point for pure H_2O;
(■) the critical point for pure NaCl.

(3600 ˚C, 260 bars), Sourirajan & Kennedy (1962) had earlier given the point (1075 "C, 930 bars). The latter is used here; the difference does not affect the qualitative descriptions, and affects the quantitative aspects significantly only at very high temperatures.

Also, for this reason, the saturation curve for pure NaCl is only roughly approximated here, by a straight line joining the triple point to the critical point.

Within the two-phase region, for a given value of T and for $p_{SAT}(T) < p < p_{CRIT}(T)$, there is a mixture of a gas phase and a liquid phase, the properties of which are determined by the NaCl mass fractions $X = X_{gs}(T, p)$ and $X = X_{\ell s}(T, p)$ for the two fluid phases respectively. The gas-phase mass fraction lies between limits, $X_{g\ SAT}(T) < X_{gs}(T, p) < X_{CRIT}(T)$, while for the liquid-phase fraction, $X_{CRIT}(T) < X_{\ell s}(T, p) < X_{\ell\ SAT}(T)$. Figures 4 and 5 show $X_{g\ SAT}(T)$ and $X_{\ell\ SAT}(T)$ respectively.

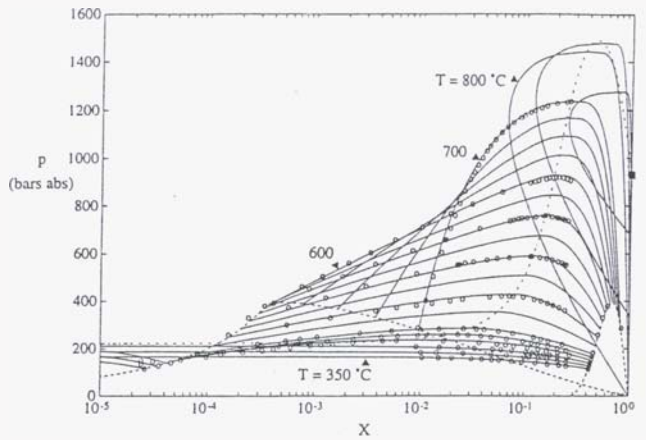

Figure 6. Correlations for the gas-phase mass fraction, $X_{gs}(T, p)$ and the liquid-phase mass fraction, $X_{\ell s}(T, p)$, of NaCl in the two-phase fluid regime. Values are plotted as isotherms for T = 350 (10) 400 (25) 700 (100) 1000 ˚C.
(o) data from Sourirajan & Kennedy (1962);
(■) the critical point for pure NaCl.

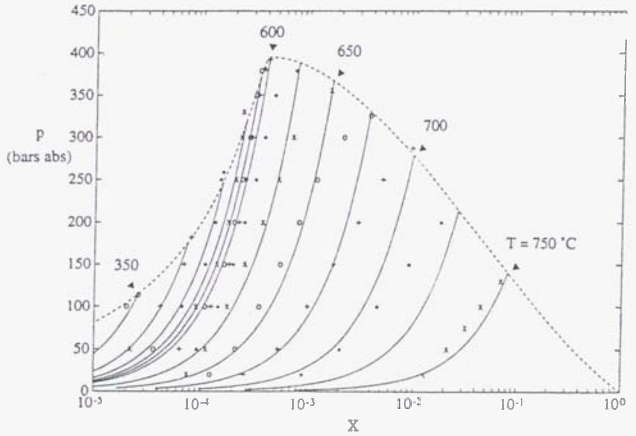

Figure 7. Correlation for the maximum solubility of halite in water vapour (gas). Values are plotted as isotherms for T = 350 (50) 600 (25) 750 "C. Corresponding marked data points are from Sourirajan & Kennedy (1962).

Figure 6 gives values of $X_{gs}(T, p)$ and $X_{\ell s}(T, p)$ as functions of p for several values of T. The curves, which coincide at $p = p_{CRIT}(T)$, are in effect isothermal cross-sections of the two-phase region boundary surface.

For this study, the remainder of the T-p-X domain is divided into regions by the above boundaries and, for T < 800 ˚ C, by the limits corresponding to the maximum solubility of NaCl in liquid water and in water vapour. The first has little variation with pressure and is therefore given approximately by $X = X_{\ell\ SAT}(T)$ for $p > p_{SAT}(T)$, while that for the solubility of NaCl in vapour (gas) is given by $X = X_{g\ sol}(T, p)$ for $p \leq p_{SAT}(T)$ (see Figure 7). The correlation is not accurate for T > 600 ˚C, but is reasonable for T ≤ 600 ˚C.

The eight regions are listed and described in Table 1. Three representative schematic isothermal cross-sections of the state-space for T < 374.15, 374.15 < T < 800 and 800 < T < 1075, are given in Figure 8, with the various regions numbered accordingly.

Table 1. State parameters for the eight different state regimes in the system H_2O-NaCl, T ≤ 1075 "C.

region	system state	T [°C]	p [bars abs]	X	S_ℓ	ε	fluid properties required
1	saturated liquid + solid	TI800	$p > p_{SAT}(T)$	$X_{\ell\,SAT}(T) \leq X < 1$	1	$0 \leq \varepsilon < 1$	$\rho_{\ell\,SAT}(T, p)$, $h_{\ell\,SAT}(T, p)$, $v_{\ell\,SAT}(T, p)$
2	supercritical liquid	T	$p \geq p_{CRIT}(T)$	$X = X_\ell$, $0 < X < X_{\ell\,SAT}(T)$	1	1	$\rho_\ell(T, p, X)$, $h_\ell(T, p, X)$, $v_\ell(T, p, X)$
3	saturated gas + solid	TI800	$p \leq p_{SAT}(T)$	$X_{g\,sol}(T, p) < X < 1$	0	$0 \leq \varepsilon < 1$	$\rho_{g\,sol}(T, p)$, $h_{g\,sol}(T, p)$, $v_{g\,sol}(T, p)$
4	subcritical gas	T	$p_{SAT}(T) < p < p_{CRIT}(T)$	$X = X_g$, $0 < X \leq X_{gs}(T, p)$	0	1	$\rho_g(T, p, X)$, $h_g(T, p, X)$, $v_g(T, p, X)$
5	two-phase gas + liquid	T	$p_{SAT}(T) < p < p_{CRIT}(T)$	$X_{gs}(T, p) < X < X_{\ell s}(T, p)$	$0 < S_\ell < 1$	1	$\rho_{\ell s}(T, p)$, $\rho_{gs}(T, p)$, $h_{\ell s}(T, p)$, $h_{gs}(T, p)$, $v_{\ell s}(T, p)$, $v_{gs}(T, p)$
6	subcritical liquid	T	$p_{SAT}(T) < p < p_{CRIT}(T)$	$X = X_\ell$, $X_{\ell s}(T, p) \leq X < X_{\ell\,SAT}(T)$	1	1	$\rho_\ell(T, p, X)$, $h_\ell(T, p, X)$, $v_\ell(T, p, X)$
7	unsaturated gas T > 800	T > 800	$p \leq p_{SAT}(T)$	$X = X_g$, $0 < X < 1$	0	1	$\rho_g(T, p, X)$, $h_g(T, p, X)$ $v_g(T, p, X)$
8	unsaturated gas T ≤ 800	T ≤ 800	$p \leq p_{SAT}(T)$	$X = X_g$, $0 < X < X_{g\,sol}(T, p)$	0	1	$\rho_g(T, p, X)$, $h_g(T, p, X)$ $v_g(T, p, X)$

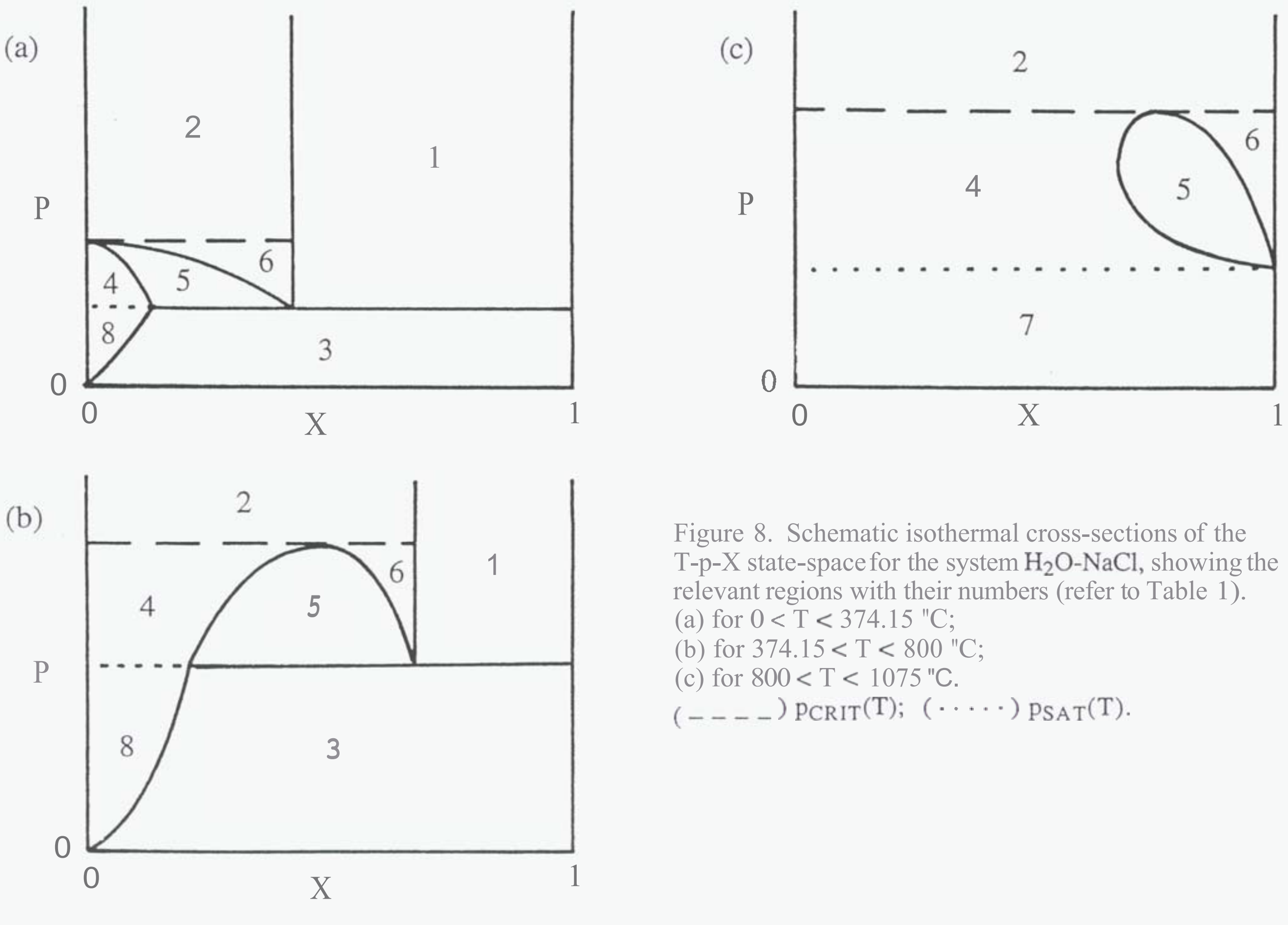

Figure 8. Schematic isothermal cross-sections of the T-p-X state-space for the system H_2O-NaCl, showing the relevant regions with their numbers (refer to Table 1).
(a) for 0 < T < 374.15 "C;
(b) for 374.15 < T < 800 "C;
(c) for 800 < T < 1075 "C.
(– – – –) $p_{CRIT}(T)$; (· · · · ·) $p_{SAT}(T)$.

3. CONSERVATION EQUATIONS

In order to follow the evolution of the system, a model mathematical description must be formulated. This can be done by using the equations describing conservation of mass, linear momentum (Darcy's law) and energy.

Conservation of mass

The transport behaviour of the fluids is firstly constrained by mass conservation requirements for each chemical ingredient. For our two-component system, these can be expressed as follows:

$$H_2O: \qquad \frac{\partial A_m^w}{\partial t} + \nabla \cdot Q_m^w = q_m^w$$

$$NaCl: \qquad \frac{\partial A_m^c}{\partial t} + \nabla \cdot Q_m^c = q_m^c$$

where

$$A_m^w = \phi\, \varepsilon\, [S_\ell(1 - X_\ell)\rho_\ell + (1 - S_\ell)(1 - X_g)\rho_g]$$

$$A_m^c = \phi\, \{(1 - \varepsilon)\rho_c + \varepsilon\, [S_\ell X_\ell \rho_\ell + (1 - S_\ell)X_g\rho_g]\}$$

are the mass per unit volume of formation of the water and chloride respectively, given in terms of the porosity ϕ, the voidage ε (volume fraction of pore space occupied by fluid), the liquid saturation S_ℓ (volume fraction of fluid occupied by liquid), the chloride mass fractions within each phase, X_ℓ and X_g, and the phase densities ρ_ℓ, ρ_g and ρ_c, where subscripts ℓ, g and c refer to liquid, gas and solid chloride respectively. The terms Q_m and q_m represent, for each component, the mass flux per unit area (see below) and the rate of injection per unit volume of mass (corresponding to a sink or source) respectively. The total mass of material per unit volume of formation is given by the sum of the respective quantities for the rock matrix, water and chloride:

$$A, = A_m^r + A_m^w + A_m^c$$

$$= (1 - \phi)\rho_r + \phi\, \{(1 - \varepsilon)\rho_c + \varepsilon\, [S_\ell\rho_\ell + (1 - S_\ell)\rho_g]\}$$

where ρ_r is the density of the solid (rock) matrix.

Conservation of momentum (Darcy's law)

The fluid fluxes are assumed to be gravity- and pressure-driven and governed by Darcy's law for porous media flow.

The mass fluxes per unit area (specific mass flow rates) are given for each component by the sum of the mass fluxes associated with each fluid phase:

$$Q_m^w = Q_{m\ell}^w + Q_{mg}^w = (1 - X_\ell)\, Q_{m\ell} + (1 - X_g)\, Q_{mg}$$

$$Q_m^c = Q_{m\ell}^c + Q_{mg}^c = X_\ell\, Q_{m\ell} + X_g\, Q_{mg}$$

Superscripts w and c refer to water and chloride respectively. Molecular diffusion of the salt is assumed small compared with advection transport and is ignored. The mass fluxes corresponding to each phase, $Q_{m\ell}$ and Q_{mg}, are given by Darcy's law applied to each phase separately, as follows:

$$Q_{m\ell} = Q_{m\ell}^w + Q_{m\ell}^c = k_{r\ell} \frac{k}{\nu_\ell}(-\nabla p + \rho_\ell g)$$

$$Q_{mg} = Q_{mg}^w + Q_{mg}^c = k_{rg} \frac{k}{\nu_g}(-\nabla p + \rho_g g)$$

Here, k is the solid matrix intrinsic permeability, $k_{r\ell}$ and k_{rg} are the relative permeabilities (permeability reduction factors which are usually dependent on S_ℓ only), ν_ℓ and ν_g are the kinematic viscosities for each fluid phase, p is the fluid pressure and g is the gravitational acceleration. The total fluid mass flux per unit area given by

$$Q_m = Q_{m\ell} + Q_{mg}$$

Conservation of energy

The equation of conservation of energy is:

$$\frac{\partial A_e}{\partial t} + \nabla \cdot Q_e = q_e$$

where q_e is a source term and

$$A_e = (1 - \phi)\rho_r u_r + \\ + \phi\, \{(1 - \varepsilon)\rho_c u_c + \varepsilon\, [S_\ell\rho_\ell u_\ell + (1 - S_\ell)\rho_g u_g]\}$$

is the energy per unit volume of the fluid-filled formation and u_r, u_c, u_ℓ and u_g are the specific internal energies for the rock matrix, solid chloride, liquid and gas phases. The energy flux per unit area Q_e is given by the sum of the energy fluxes corresponding to the flow of each phase and that due to heat conduction, as follows:

$$Q_e = Q_{m\ell}\, h_\ell + Q_{mg}\, h_g - K\, \nabla T$$

where $Q_{m\ell}$ and Q_{mg} are given above, h_ℓ and h_g are the specific enthalpies of the liquid and gas fluid phases, and K is the effective thermal conductivity of the fluid-filled formation.

Dissolution of chloride

Associated with precipitation and redissolving of solid chloride is an amount of energy, the heat of solution. In general, this will depend on whether the solid is in equilibrium with the liquid or gas form of the fluid.

$$u_{fluid}^c = u_c + u_{solution}^c$$

Mixture quantities

The above equations require a knowledge of various fluid properties. Some fluid properties for a general liquid-gas mixture are given by:

mixture density ρ:

$$\rho = S_\ell\rho_\ell + (1 - S_\ell)\rho_g$$

specific internal energy u:

$$\rho u = S_\ell\rho_\ell u_\ell + (1 - S_\ell)\rho_g u_g$$

mixture enthalpy h:

$$\rho h = S_\ell \rho_\ell h_\ell + (1 - S_\ell)\rho_g h_g$$

where the separate phase properties ρ_ℓ, ρ_g, u_ℓ, u_g, h_ℓ and h_g are all functions of T, p and X. Note that internal energies can be calculated from the state variables and values of specific enthalpies and densities by

$$h_g = u_g + \frac{p}{\rho_g}, \quad h_\ell = u_\ell + \frac{p}{\rho_\ell}, \quad h = u + \frac{E}{\rho}$$

The independent fluid properties required within each region of the state-space, and their functional dependence, are listed in Table 1.

Determination of the voidage ε and the liquid saturation S_ℓ for the two-phase regimes

The mass fraction X of chloride within the pore fraction of the system is given by

$$X = \frac{A_m^c}{A_m^w + A_n^c}$$

$$= \frac{(1-\varepsilon)\rho_c + \varepsilon[S_\ell X_\ell \rho_\ell + (1-S_\ell)X_g\rho_g]}{(1-\varepsilon)\rho_c + \varepsilon[S_\ell\rho_\ell + (1-S_\ell)\rho_g]}$$

In regions 2, 4, 6, 7 and 8 of the T-p-X state-space, $\varepsilon = 1$ and either $S_\ell = 1$ or $S_\ell = 0$ and X is just the mass fraction of chloride within the liquid or gas (see Table 1). Within regions 1, 3 and 5, the above expression can be inverted to give ε, ε and S_ℓ respectively as functions of X. The corresponding inversion formulas are as follows:

Region 1 (liquid + solid)

$$\varepsilon = \frac{(1-X)\rho_c}{(1-X)\rho_c + (X - X_{\ell SAT})\rho_{\ell SAT}}$$

Region 2 (gas + solid)

$$\varepsilon = \frac{(1-X)\rho_c}{(1-X)\rho_c + (X - X_{gsol})\rho_{gsol}}$$

Region 3 (gas + liquid)

$$S_\ell = \frac{(X - X_{gs})\rho_{gs}}{(X_{\ell s} - X)\rho_{\ell s} + (X - X_{gs})\rho_{gs}}$$

This means that T, p and X can be used to determine the state of the system within all regions. The boundaries X = 0 and X = 1, which correspond to pure H20 and pure NaCl, are not included in this classification.

ACKNOWLEDGEMENTS

This research was supported by contract number MPR201 between Maths Physics Research Limited and the Foundation for Research, Science & Technology. The work was assisted by interactions with Steve White, staff from the Department of Engineering Science at the University of Auckland, and by the blessing and encouragement of the Department of Mathematics, Massey University.

APPENDIX

Correlation formulas

Saturation surface (Figure 2) For T < 800,

$$p_{SAT}(T) = a_1 t + a_2 t^2 + a_3 t^3 + a_4 t^4 + a_5 t^5$$

where $t = (T/800)^2$, while, for 800 ≤ T ≤ 1075,

$$p_{SAT}(T) = 930\,\frac{T - 800}{1075 - 800}$$

(the saturation curve for pure NaCl)

Critical curve (Figure 3) For T < 374.15,

$$X_{CRIT}(T) = 0$$
$$p_{CRIT}(T) = p_{sat}(T)$$

(the saturation curve for pure H_2O),
while, for 374.15 ≤ T ≤ 1075,

$$X_{CRIT}(T) = b_0 + b_1 T + b_2 T^2 + b_3 T^3$$
$$p_{CRIT}(T) = c_0 + c_1 T + c_2 T^2 + c_3 T^3$$

Saturation curve: gas (Figure 4) For T < 600,

$$X_{g\,SAT}(T) = 10^{-(d_0 + d_1 T + d_2 T^2 + d_3 T^3)}$$

while, for 600 ≤ T < 800,

$$X_{g\,SAT}(T) = 10^{-(e_0 + e_1 T + e_2 T^2)}$$

and, for 800 ≤ T ≤ 1075,

$$X_{g\,SAT}(T) = 1$$

Saturation curve: liquid (Figure 5) For T < 800,

$$X_{\ell\,SAT}(T) = f_0 + f_1 T + f_2 T^2$$

while, for 800 ≤ T ≤ 1075,

$$X_{\ell\,SAT}(T) = 1$$

Gas + liauid region boundary surfaces: liquid (Figure 6)

For $p_{SAT}(T) < p < p_{CRIT}(T)$,

$$X_{\ell s}(T, p) = X_{CRIT}(T)\left\{\frac{X_{\ell\,SAT}(T)}{X_{CRIT}(T)}\right\}^{\left[\frac{p_{CRIT}(T) - p}{p_{CRIT}(T) - p_{SAT}(T)}\right]^z}$$

where $$z = \left\{1 - \frac{1.4\log_{10}[X_{CRIT}(T)]}{1 + 80a} + 6a\right\}^{-1}$$

with, for T ≤ 374.15,

$$a = 0$$

and, for $374.15 < T \leq 1075$,

$$a = \left(\frac{T}{800}\right)^2 - \left(\frac{374.15}{800}\right)$$

Gas + liquid region boundary surfaces: gas (Figure 6)

For $p_{SAT}(T) < p < p_{CRIT}(T)$,

$$X_{gs}(T, p) = b\, X_{CRIT}(T) \left\{\frac{X_{g\ SAT}(T)}{X_{CRIT}(T)}\right\}^{\left[\frac{p_{CRIT}(T) - p}{p_{CRIT}(T) - p_{SAT}(T)}\right]^z}$$

where, for $T \leq 374.15$,

$$b = 1$$

and $$z = \left\{1 - 1.4 \log_{10}[X_{CRIT}(T)]\right\}^{-1}$$

and, for $374.15 < T \leq 1075$,

$$b = 10^{\,g\left\{\left[\frac{p_{CRIT}(T) - p}{p_{CRIT}(T) - p_{SAT}(T)}\right] - \left[\frac{p_{CRIT}(T) - p}{p_{CRIT}(T) - p_{SAT}(T)}\right]^{\frac{1}{2}}\right\}}$$

with

$$g = 2 + \frac{4}{3} t_g \frac{1 - t_g{}^2}{t_g{}^2 + 5/27}, \quad \text{where} \quad t_g = \frac{T - 700}{300}$$

and $$z = 1.$$

Solid solubility in gas (Figure 7)

For $T < 800$ and $p \leq p_{SAT}(T)$,

$$X_{g\ sol}(T, p) = X_{g\ SAT}(T)\, \frac{p}{p_{SAT}(T)}$$

Correlation coefficients

i	0	1	2	3	4	5
a_i		-1.82713e+1	4.34823e+3	-5.78297e+3	-5.27604e+2	1.98062e+3
b_i	7.86714e+2	-6.96490e+0	1.88317e-2	-1.13756e-5		
c_i	-1.02936e+0	4.86486e-3	-7.18666e-6	4.10909e-9		
d_i	1.43797e+1	-5.01938e-2	7.79367e-5	-4.13778e-8		
e_i	-2.03949e+0	2.85018e-2	-3.24406e-5			
f_i	2.6218e-1	7.2e-5	1.06e-6			

REFERENCES

Anderson, G., Probst, A,, Murray, L. and Butler, S. An accurate PVT model for geothermal fluids as represented by H_2O-CO_2-NaCl mixtures. *Proc. Seventeenth Workshop Geothermal Reservoir Engineering,* Stanford University, 1992.

Bischoff, J.L. Densities of liquids and vapours in boiling NaCl-H_2O solutions: a PVTx summary from 300 "C to 500 "C. *American J. Sci.* 291, 309-338, 1991.

Bischoff, J.L. and Pitzer, K.S. Liquid-vapor relations for the system NaCl-H_2O: Summary of the P-T-x surface from 300 "C to 500 "C. *American J. Sci.* 289, 217-248, 1989.

Bowers, T.S. and Helgeson, H.C. Calculation of the thermodynamic and geochemical consequences of nonideal mixing in the system H_2O-CO_2-NaCl on phase relations in geologic systems: Equation of state for H_2O-CO_2-NaCl fluids at high pressures and temperatures. *Geochim. Cosmochim. Acta* 47, 1247-1275, 1983.

Chou, I-M. Phase relations in the system NaCl-KCl-H_2O. III: Solubilities of halite in vapor-saturated liquids above 445 "C and redetermination of phase equilibrium properties in the system NaCl-H_2O to 1000 "C and 1500 bars. *Geochim. Cosmochim. Acta* 51, 1965-1975, 1987.

Haas, J.L. Jr. Physical properties of the coexisting phases and thermochemical properties of the H20 component in boiling NaCl solutions: Preliminary steam tables for NaCl solutions. *Geological Survey Bull.* 1421-A, 1976.

McNabb, A. The Taupo-Rotorua hot-plate. *Proc. 14th New Zealand Geothermal Workshop 1992,* University of Auckland, 111-114, 1992.

Rogers, G.F.C. and Mayhew, Y.R. *Thermodynamic and transport properties of fluids.* 3rd ed. Blackwell, 1980.

Sourirajan, S. and Kennedy, G.C. The system H_2O-NaCl at elevated temperatures and pressures. *American* J. *Sci.* 260, 115-141, 1962.